

# Preparation and dielectric properties of $\text{BaBi}_{1.8}\text{Ln}_{0.2}\text{Nb}_2\text{O}_9$ (Ln = Ce, Gd) ceramics

MOHAMED AFQIR<sup>1,2,\*</sup>, AMINA TACHAFINE<sup>2</sup>, DIDIER FASQUELLE<sup>2</sup>, MOHAMED ELAATMANI<sup>1</sup>,  
JEAN-CLAUDE CARRU<sup>2</sup>, ABDELOUAHAD ZEGZOUTI<sup>1</sup>, MOHAMED DAOUD<sup>1</sup>

<sup>1</sup> Laboratoire des Sciences des Matériaux Inorganiques et leurs Applications, Faculté des Sciences Semlalia, Université Cadi Ayyad, Marrakech, Maroc

<sup>2</sup> Unité de Dynamique et Structure des Matériaux Moléculaires, Université du Littoral- Côte d'Opale, Calais, France

The main subject of the presented research is to investigate the dielectric properties of  $\text{BaBi}_{1.8}\text{Ln}_{0.2}\text{Nb}_2\text{O}_9$  (Ln = Ce, Gd) ceramics prepared by conventional solid state reaction route. The materials were examined using XRD and FT-IR methods. Moreover, the AC conductivity, dielectric constant and dielectric loss of the ceramics were determined. X-ray diffraction confirmed that all these compounds crystallize in an orthorhombic structure. Fourier transform infrared spectroscopy study confirmed the presence of two characteristic vibration bands located at around  $617\text{ cm}^{-1}$  and  $818\text{ cm}^{-1}$  for  $\text{BaBi}_2\text{Nb}_2\text{O}_9$ . The experimental results show that the substitution of Bi by Ce or Gd causes a decrease in Curie temperature, dielectric constant and dielectric loss.

Keywords:  $\text{BaBi}_2\text{Nb}_2\text{O}_9$ ; structure; dielectrics

## 1. Introduction

Aurivillius bismuth-layer structured ferroelectrics (BLSFs), owing to their excellent dielectric and piezoelectric properties, are attractive for a wide range of applications such as ferroelectric non-volatile random access memory (FeRAM) storage devices over a wide range of temperatures [1].  $\text{BaBi}_2\text{Nb}_2\text{O}_9$ ,  $\text{SrBi}_2\text{Nb}_2\text{O}_9$  and  $\text{SrBi}_2\text{Ta}_2\text{O}_9$  are several bismuth-layer compounds which suffer from high dielectric loss, due to volatilization of bismuth. To solve more or less this problem, many researches proposed to substitute bismuth by lanthanide [2–4], what has been presented in our earlier paper [5].  $\text{SrBi}_2\text{Nb}_2\text{O}_9$  and  $\text{SrBi}_2\text{Ta}_2\text{O}_9$  are superior candidates for new generation of ferroelectric random-access memories (FeRAM) in comparison to  $\text{BaBi}_2\text{Nb}_2\text{O}_9$  [6]. To the best of our knowledge, there has been lack of sufficient information about rare-earth-doped  $\text{BaBi}_2\text{Nb}_2\text{O}_9$  ceramics. In this paper,  $\text{BaBi}_{1.8}\text{Ln}_{0.2}\text{Nb}_2\text{O}_9$  (Ln: Ce and Gd) samples were

synthesized through a solid-state reaction method. In addition, structural and dielectric responses were investigated.

## 2. Experimental

Synthesis of the materials was performed starting from stoichiometric amounts of  $\text{Bi}_2\text{O}_3$  (Rectapur, 99 %),  $\text{BaCO}_3$  (Acros Organics, 90 %),  $\text{Nb}_2\text{O}_5$  (Acros Organics, 99.5 %),  $\text{Ce}_2\text{O}_3$ , and  $\text{Gd}_2\text{O}_3$  (Alfa Aesar, 99.99 %). The stoichiometric amounts of the raw materials were thoroughly ground manually in a mortar for one hour and then calcined for 12 hours at  $1100\text{ }^\circ\text{C}$ . The samples were then uniaxially pressed at 2 MPa into pellets having 6 mm in diameter. The pellets were covered with powders of the same materials and heated for 8 hours at  $1150\text{ }^\circ\text{C}$ . The powder ceramics were characterized by X-ray diffraction with a powder diffractometer (PANalytical/Philips X'Pert) and infrared spectroscopy (KBr-pellet/Bruker, Vertex 70 DTGS). For dielectric measurements, both the surfaces of pellets were painted uniformly with a silver conductive paste (Alfa Aesar) and cured for 1 hour

\*E-mail: mohamed.afqir@yahoo.fr

at 400 °C. The temperature dependence of dielectric properties was measured at temperature ranging from room temperature to 500 °C using an LCR meter HP 4284A (Hewlett Packard Co).

### 3. Result and discussion

Fig. 1 shows X-ray diffraction patterns of pure and doped  $BaBi_2Nb_2O_9$ . According to the standard pattern of  $BaBi_2Nb_2O_9$  (PDF #00-049-0607), all the observed reflections could be indexed to orthorhombic structure. The highest peak corresponding to (1 1 5) orientation is consistent with the (1 1 2m+1) highest diffraction peak in bismuth-layered structured ferroelectric systems [7]. Table 1 shows the effect of Ce and Gd on the crystal structure. The values  $a$ ,  $b$ ,  $c$ ,  $V$  and their experimental error have been calculated using the UnitCell program. It can be seen that the values of  $c$  are much higher than the values of  $a$  and  $b$  which implies that the crystal structure is anisotropic. It can be seen that the unit cell volume decreases with a decrease in the ionic radius (ionic radii of  $Gd^{3+}$ ,  $Ce^{3+}$  and  $Bi^{3+}$  are 0.938 Å, 1.034 Å and 1.02 Å, respectively), indicating that these cations have diffused into the  $BaBi_2Nb_2O_9$  lattice.

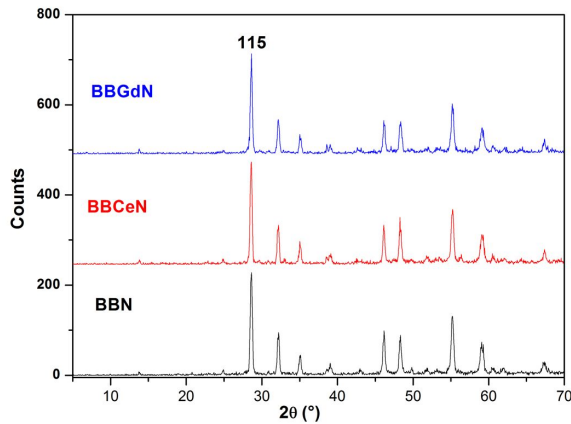


Fig. 1. XRD patterns of the Ln-doped  $BaSrBi_2Nb_2O_9$  ceramic powders.

FT-IR transmittance spectra of these powders are shown in Fig. 2. A broad band around  $\sim 3442\text{ cm}^{-1}$  is assigned to the O–H stretching vibrations of adsorbed water molecules

present in the sample. Around  $\sim 2933\text{ cm}^{-1}$  and  $\sim 1625\text{ cm}^{-1}$  the band is assigned to the C–H stretching and bending vibrations, respectively. A band at  $\sim 2360\text{ cm}^{-1}$  relates to  $CO_2$ . The bands at  $1420\text{ cm}^{-1}$ ,  $1060\text{ cm}^{-1}$  are assigned to carbonate. Two bands are noted around  $\sim 617\text{ cm}^{-1}$  and  $\sim 818\text{ cm}^{-1}$  which are respectively assigned to the symmetric and asymmetric stretching of the Nb–O bond in the  $NbO_6$  octahedral. These two bands are characteristic of niobates  $ABi_2Nb_2O_9$  ( $A = Sr, Ca, Ba, Pb$ ) [8–10]. It is found that FT-IR spectra of this species show a strong resemblance. Thus, Ce or Gd substitution will not have a significant enough effect on the shifts in frequencies.

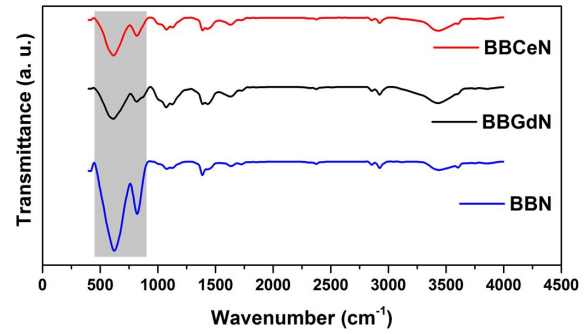


Fig. 2. FT-IR spectra of Ln-doped  $BaBi_2Nb_2O_9$  ceramic powders.

Fig. 3 shows dielectric constant  $\epsilon'$  and loss tangent  $\tan\delta$  of Ce and Gd-doped  $BaBi_2Nb_2O_9$  ceramics as a function of temperature at measurement frequencies of  $10^2\text{ Hz}$ ,  $10^3\text{ Hz}$  and  $10^4\text{ Hz}$ . The relationship between the real  $\epsilon'$  and imaginary  $\epsilon''$  parts of the complex dielectric constant and loss tangent  $\tan\delta$  are expressed by the following relations:

$$\epsilon' = \frac{Cd}{A\epsilon_0} \quad (1)$$

$$\epsilon'' = \epsilon' \tan \delta \quad (2)$$

where  $C$  is the capacitance,  $d$  is the pellet thickness,  $A$  is the electrode area, and  $\epsilon_0$  is the permittivity of free space ( $\epsilon_0 = 8.85 \times 10^{-12}\text{ F/m}$ ).

Table 1. Lattice parameters of Ce and Gd-doped BaBi<sub>2</sub>Nb<sub>2</sub>O<sub>9</sub>.

	BBN	BBCeN	BBGdN
a [Å]	5.602±0.00108	5.595±0.00108	5.551±0.00108
b [Å]	5.630±0.00028	5.67±0.00028	5.562±0.00028
c [Å]	25.481±0.00174	25.556±0.00174	25.669±0.00174
V [Å] <sup>3</sup>	803.652±0.1411	810.730±0.1412	792.522±0.1412

The Curie temperatures ( $T_C$ ) have been found at about 340 °C, 330 °C and 310 °C for BBN, BBGdN and BBCeN, respectively. The peak value of dielectric constant ( $\epsilon'_{\max}$ ) is 1544 for BBN, which is higher than that of BBGdN (228) and BBCeN (485), when measured at 1 kHz. The loss tangent increases with an increase in the temperature and reaches to local maximum at 335 °C, 330 °C and 310 °C for BBN, BBGdN and BBCeN, respectively. This loss tangent additionally confirms the phase transition from ferroelectric to paraelectric phase at the Curie temperature. The values of  $\tan\delta$  at room temperature decreases from 0.1 (BBN) to  $\sim 0.06$  (Ln-doped BBN) when measured at 10 kHz.

The Curie temperature obtained for the BBN ceramics is comparable to those previously reported in the literature [11]. The significant reduction of  $\epsilon'_{\max}$  may be explained by macroscopic Clausius-Mossotti relationship and polarizabilities as given by Shannon [12] ( $\alpha_{\text{Bi}}^{3+} = 6.12 \text{ \AA}^3$ ,  $\alpha_{\text{Gd}}^{3+} = 4.37 \text{ \AA}^3$ ,  $\alpha_{\text{Ce}}^{3+} = 6.15 \text{ \AA}^3$ ).

Fig. 4 shows Curie-Weiss fittings of dielectric constant at 1 kHz according to equation 3:

$$\epsilon' = \frac{C}{T - T_{CW}} \quad (3)$$

where  $C$  is the Curie constant and  $T_{CW}$  is the Curie-Weiss temperature, which differs from the Curie temperature. The magnitude of the Curie constant is of about  $10^5 \text{ }^\circ\text{C}$ , indicating the displacive nature of the observed transition. The ratio of the Curie constants above and below the phase transition is equal to 1 for SBCeN, which is of the same order as for SBGdN, but smaller than BBN ( $\sim 1.3$ ), referring to the first-order ferroelectric phase transition.

Fig. 5 shows the dependence of AC conductivity on inverse of temperature at 1 kHz. The curve was fitted with Arrhenius equation:

$$\sigma = \omega \epsilon_0 \epsilon' \tan \delta = \sigma_0 e^{-\frac{E_a}{k_B T}} \quad (4)$$

where  $E_a$  is the activation energy,  $k_B$  is the Boltzmann constant and  $\sigma_0$  is pre-exponential factor. In the lower temperature region ( $3.5 \text{ K}^{-1}$  to  $2.5 \text{ K}^{-1}$ ), conductivity shows a weak temperature dependence. In the higher temperature region ( $2.5 \text{ K}^{-1}$  to  $1 \text{ K}^{-1}$ ), conductivity shows a strong temperature dependence.

The activation energy calculated from the slope of the curve in the inset (Fig. 5) is found to be 1.06 eV, 0.95 eV and 0.69 eV for BBN, BBCeN and BBGdN, respectively, when measured at 1 kHz. A decrease in activation energy may be attributed to the presence of  $\text{Ce}^{3+}$  and  $\text{Gd}^{3+}$  ions in the lattice, which reduce the oxygen vacancy formation. The bond dissociation energy of Gd–O (353 kJ/mol) Ce–O (353 kJ/mol) is larger than that of Bi–O (343 kJ/mol) [12, 13]. Hence, the substitution of Bi by Ce or Gd suppresses the formation of oxygen vacancies.

In the light of the above mentioned, BBN ceramics shows high values of  $\tan\delta$ , what restricts its practical applications. On the other hand, the Ce and Gd-doped BBN ceramics show dielectric properties, which are desirable in nonvolatile FeRAM applications.

## 4. Conclusions

BaBi<sub>1.8</sub>Ln<sub>0.2</sub>Nb<sub>2</sub>O<sub>9</sub> (Ln = Ce, Gd) samples have been prepared by the solid-state reaction method. The XRD patterns showed the presence of the parent BaBi<sub>2</sub>Nb<sub>2</sub>O<sub>9</sub> phase. The difference observed in unit cell parameters has been correlated with the ionic radius. The appearance of Nb–O vibration bands in FT-IR spectra is characteristic of barium bismuth niobate phase formation.

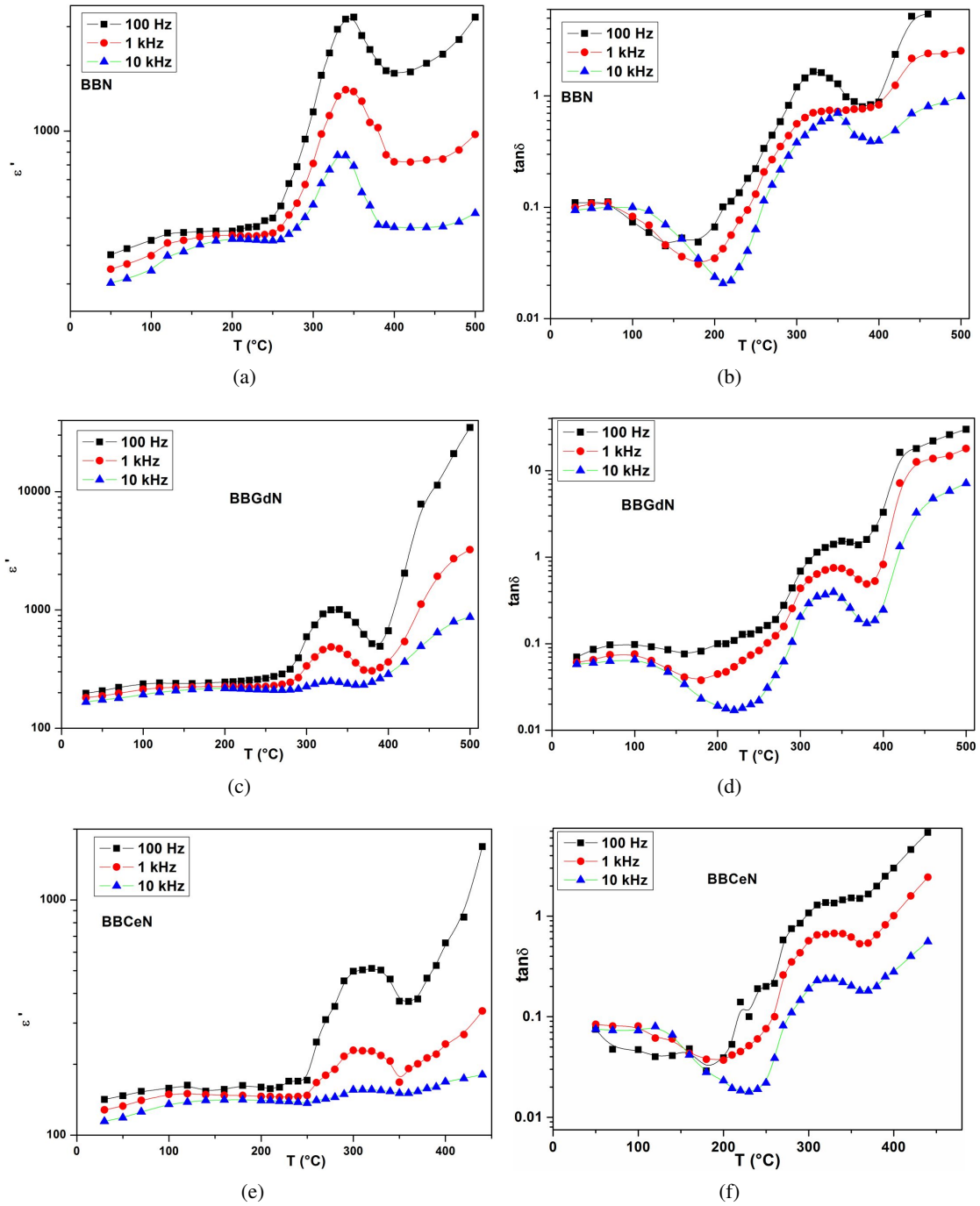


Fig. 3. Temperature dependence of dielectric constant  $\epsilon'$  and loss tangent  $\tan\delta$  of Ln-doped  $BaBi_2Nb_2O_9$  ceramics.

Dielectric measurements revealed a decrease in the Curie temperature from 340 °C for BBN to 330 °C and 310 °C for BBCeN and BBGdN respectively. The dielectric constant  $\epsilon'$  and loss tangent  $\tan\delta$  of pure

$BaBi_2Nb_2O_9$  are higher than those of Ce and Gd-doped  $BaBi_2Nb_2O_9$  ceramics. Moreover, the reduction in the dielectric loss  $\tan\delta$  may be attributed to suppression of oxygen vacancies by the cationic vacancies created by cerium and

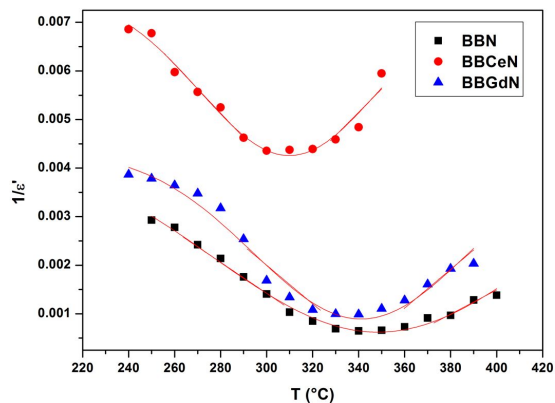


Fig. 4. Temperature dependence of reciprocal dielectric constant.

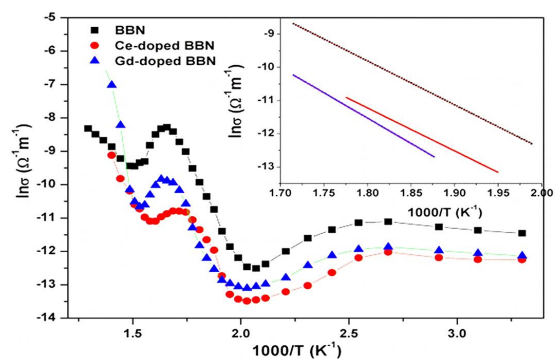


Fig. 5. Conductivity in an Arrhenius plot for Ln-doped BBN at 10 kHz. The inset shows the variation of the conductivity data fitting in the 95 °C to 105 °C temperature range.

gadolinium doping. These results are useful for the potential applications of  $\text{BaBi}_{1.8}\text{Ln}_{0.2}\text{Nb}_2\text{O}_9$  (Ln = Ce, Gd) ceramics.

## References

- [1] PARK B.H., KANG B.S., BU S.D., NOH T.W., LEE J., JO W., *Nature.*, 401 (1999), 682.
- [2] SHRIVASTAVA V., JHA A.K., MENDIRATTA R.G., *Mater. Lett.*, 60 (2006), 1459.
- [3] SUN L., CHU J.-H., YANG P.-X., YUE F.-Y., LIU Y.-W., FU C.-D., MAO C.-L., *Trans. Nanoferrous Met. Soc. China.*, 19 (6) (2009), 1459.
- [4] ZOU H., YU Y., LI J., CAO Q., WANG X., HOU J., *Mater. Res. Bull.*, 69 (2015), 112.
- [5] AFQIR M., TACHAFINE A., FASQUELLE D., ELAATMANI M., CARRU J., ZEGZOUTI A., DAUD M., *Process. Appl. Ceram.*, 3 (2016), 183.
- [6] LAHA A., KRUPANIDHI S.B., *J. Appl. Phys.*, 92 (2002), 415.
- [7] SARAH P., *Procedia Eng.*, 10 (2011), 2684.
- [8] KASPROWICZ D., LAPINSKI A., RUNKA T., SPEGHINI A., BETTINELLI M., *J. Alloy. Compd.*, 478 (2009), 30.
- [9] ROCHA DA M.J.S., FILHO M.C.C., THEOPHILO K.R.B., DENARDIN J.C., VASCONCELOS DE I.F., ARAUJO DE E.B., SOMBRA A.S.B., *Mater. Sci. Appl.*, 3 (1) (2012), 6.
- [10] RAMARAGHAVULU R., BUDDHUDU S., *Ferroelectrics.*, 460 (2014), 57.
- [11] ADAMCZYK M., UJMA Z., PAWE M., SZYMCZAK L., *J. Mater. Sci.*, (2006), 79 (2006) 435.
- [12] SHANNON R.D., *J. Appl. Phys.*, 73 (1993) 438.
- [13] WU Y., CAO G., *Mater. Res. Soc.*, 15 (2000), 1583.
- [14] COTTRELL T.L., *The Strengths of Chemical Bond*, Hardcover, 1958.

Received 2017-02-25

Accepted 2018-02-17